ACTA ABP BIOCHIMICA POLONICA

Vol. 69, No 3/2022
513–522
https://doi.org/10.18388/abp.2020_6432

Regular paper

Comparison of metabolic effects of mitochondrial dysfunctions in the context of vulnerability to fatigue: computer simulation study*

Michał J. Sabat✉

Department of Biophysics, Faculty of Biochemistry, Biophysics and Biotechnology Jagiellonian University, Kraków, Poland

In recent years, the accumulation of phosphate ions and the increase in acidity have been described as crucial metabolic fatigue-leading factors that disturb muscle fiber contractions. This fact is especially important in the context of mitochondrial dysfunctions in which excessive fatigue is one of the possible symptoms. However, little is known about the precise fatigue-inducing thresholds of work intensity in mitochondrial dysfunctions of various types and at various stages of their severity. Possible interactions of additional factors such as disturbances in electrolyte concentrations (i.e. magnesium ions) were also not precisely defined. One of the best-suited tools for this kind of problem is systems biology, which enables modeling of metabolic pathways. In this research, a computer model of working skeletal muscle was adapted. The relationship between the decrease in oxidative phosphorylation and the workload shows a linear dependence for dysfunctions that evenly disturb the activity of each element of the pathway (which is equivalent to the decrease in mitochondrial mass). In case of dysfunctions that disrupt only one element of the pathway, the relationship between fatigue threshold and exercise intensity is exponential, but with higher threshold deficiency values. Muscle phosphate levels were the most vulnerable to disruptions of complex III and ATP synthase. Surprisingly, disruptions of the ATP/ADP exchanger emerged as equally disruptive and capable of significantly increasing phosphate concentrations also in the rest state, whereas the impact of the impairment of the phosphate transporter was negligible. Perturbations in magnesium concentration also did not show a significant effect in any of these models.

Keywords: Skeletal muscle, exercise intolerance, phosphate accumulation, magnesium, adenine nucleotide translocator (ANT), computer model

Received: 01 April, 2022; revised: 01 July, 2022; accepted: 19 July, 2022; available on-line: 01 September, 2022

✉e-mail: michal.sabat@student.uj.edu.pl

*__Preliminary report information__: Factors of skeletal muscle fatigue and excessive vulnerability to fatigue in mitochondrial diseases in the light of systems biology M. J. Sabat, XLIX FBBB Winter School 2021. Changes in metabolites concentrations leading to excessive fatigue in mitochondrial diseases. Theoretical study with aid of skeletal muscle oxidative phosphorylation model. M. J. Sabat, B. Korzeniewski XLVII FBBB Winter School 2019

Abbreviations: A_{UT}, Multiple of ATP Utilization; CI-IV, Electron Transport Chain Complex I-IV; ETC, Electron Transport Chain; EX, ATP/ADP Exchanger; OXPHOS, Oxidative Phosphorylation; P_i, Inorganic Phosphate; PI, Mitochondrial Phosphate Transporter (Importer); SN, ATP Synthase; $\dot{V}O_2$, Oxygen Uptake Rate

INTRODUCTION

Among the factors that describe human physical abilities, one of the most crucial is endurance against fatigue. Closely related to this phenomenon is the critical power parameter. Physical effort within the limits of this threshold could be sustained. The workload above the values of this parameter could be kept only for a given time, inevitably resulting in the cessation of muscle work and the inability to restore it (Poole *et al.,* 2016). That exact process is known as muscle fatigue or peripheral fatigue. There exists also the phenomenon of central fatigue, which encompasses the problems of maintaining the nerve stimulation necessary for muscle contractions (Gandevia, 2001). However, the central fatigue is outside of the scope of this work.

The question of the mechanisms that lead to muscle fatigue has been the subject of extensive research (Debold *et al.,* 2012; Nelson *et al.,* 2014; Jarvis *et al.,* 2018; Woodward & Debold, 2018). Increased cytoplasmic acidity and accumulation of phosphate ion concentration were postulated to be the main fatigue-leading factors (Woodward & Debold, 2018; Sundberg *et al.,* 2019). Both H^+ and Pi ions are capable of perturbing muscle contractions in various (sometimes interdependent) ways and at various levels. Possible mechanisms consist of interaction with calcium ion influx, interference with the initiation of the Ca^{2+}-troponin interaction, disruption of the process of myosin attachment to actin fibers, and slowdown of myosin enzymatic activity and movement. Exact mechanisms were described in (Debold *et al.,* 2016; Cheng *et al.,* 2018; Sundberg & Fitts, 2019).

Another factor commonly associated with fatigue were magnesium ions. Apart from its impact on various mechanisms such as oxygen transport by erythrocytes, muscle nerve stimulation, calcium efflux from the sarcoplasmic reticulum, and defense against ROS, hypothetically, magnesium might also interact with pH- and phosphate-dependent mechanisms of fatigue (Nielsen & Lukaski, 2006). This might also occur at the level of metabolite accumulation. For example, through the known process of complex formation between Mg^{2+} ions and ATP or ADP (Murphy, 2000) magnesium might influence the rate of transformations of these nucleotides and, thus, possibly lead to changes in the rate of accumulation of phosphate or H^+ ions.

For phosphate, 25 mM could be assumed as the threshold concentration according to the work of Korzeniewski (Korzeniewski, 2019). In that work, adopting such a threshold value resulted in simulation data well fitted to the *in vivo* experimental results. The publication by Debold and others (Debold *et al.,* 2016).

also points to phosphate concentrations in the range of 25–30 mM as the factor disrupting work of the muscle fibers. It also presents phosphate as the main fatigue-leading factor. Fatigue-related values for *in vivo* experiments range from 22.7 to 32.3 mM (Sundberg *et al.,* 2019). In the case of acidity, the assumed threshold pH is equal to 6.6. According to the literature, the pH must fall at least below the level of 6.7 to start the fatigue-inducing perturbations of muscle work (Fitts, 2008). Sundberg and Fitts (Sundberg & Fitts, 2019) list the pH values between 6.67 and 6.5 as fatigue-related levels.

The accumulation of phosphate ions and the increase in acidity in myocytes are consequences of the work of bioenergetic pathways under conditions of increased ATP demand. Thus, critical power could be seen as the ATP threshold demand above which accumulation of phosphate and eventually H^+ starts the positive feedback loop of the perturbed efficiency of the muscle work and its compensation by further increase in the demand for ATP (Korzeniewski, 2019). The main sources of ATP for myocytes are aerobic and 'anaerobic' glycolysis, the Krebs cycle-powered oxidative phosphorylation system, buffering of ATP levels by phosphocreatine and creatine kinase, and the activity of adenylate kinase. Adenylate kinase transforms two ADP molecules into one molecule of ATP and one molecule of AMP. Among the pathways mentioned above, some result in additional mobilization of phosphate, which is further freed by ATP consumption (Korzeniewski, 2016). Part of these processes also perturb cytosolic pH levels (Robergs *et al.,* 2004). Obviously, this must not be confused with the common incorrect presumption about the alleged acidifying effect of lactic acid on the muscle (Robergs *et al.,* 2004; Hall *et al.,* 2016). Additionally, to explain the ability of myocytes to sustain a high demand for ATP in time of severe exercise, the phenomenon of an additional boost in the intensity of oxidative phosphorylation was postulated. One of the most probable mechanisms of this process is the so-called *Each-Step Activation* (ESA). This mechanism assumes a proportional increase in the activity of all mitochondrial electron transport chain complexes together with ATP synthase (Korzeniewski & Rossiter, 2015; Korzeniewski, 2017).

Perturbations in any of these bioenergetic pathways could lead to the accumulation of P_i or H^+ in the cytosol (Korzeniewski, 2016). Obstacles to the proper flow of metabolites could result from both decreased enzyme activities and impaired functioning of metabolite carriers such as the ATP/ADP exchanger or the phosphate (and H^+) transporter. These perturbations are especially pronounced in the case of mitochondrial diseases (Korzeniewski, 2015; Korzeniewski, 2016). Various mitochondrial dysfunctions could disrupt the functioning of the whole or of the individual parts of the oxidative phosphorylation system (further abbreviated as OXPHOS) – the main source of ATP for the working muscle (Sharp & Haller, 2014; Korzeniewski, 2015; Kanungo *et al.,* 2018). Alternatively, depletion of the pool of functional mitochondria can give equivalent results. These disturbances may lead to an excessive accumulation of phosphate and acidity, resulting in increased vulnerability to fatigue. This vulnerability is one of the common symptoms of mitochondrial diseases, and its severity can depend on the character of the given mitochondrial dysfunction or the stage of its development (Korzeniewski, 2015; Korzeniewski, 2016; Korzeniewski, 2019). However, research on the wide comparisons of dependence between the degree of impairment of given elements of OXPHOS and the corresponding fatigue thresholds is lacking. The aim of this research is to try to answer this problem through a systems biology approach. For this purpose, the computer model of the skeletal muscle bioenergetic system developed by Bernard Korzeniewski and others (Korzeniewski & Rossiter 2015; Korzeniewski & Zoladz, 2015; Korzeniewski, 2017) was applied. Modifications to the reaction rate parameters of this model allowed the simulation of multiple stages and types of impairment of the OXPHOS system in situations of various workload intensities and additional metabolic disturbances.

COMPUTER MODEL AND METHODOLOGY

The computer model of the bioenergetic systems of skeletal muscle applied in this research was developed and gradually validated by Bernard Korzeniewski and others (Korzeniewski & Rossiter, 2015; Korzeniewski & Zoladz, 2015; Korzeniewski, 2017). The model consists mainly of the oxidative phosphorylation system (OXPHOS) that encompasses mitochondrial electron transport chain (ETC) Complexes I, III, and IV (CI, CIII, CIV), ATP synthase (SN), ATP/ADP exchanger (EX) and phosphate carrier (PI). Pools of reduced - and oxidized electron carriers of the mitochondrial electron transport chain, ubiquinone, and cytochrome *c*, were also modeled. However, glycolysis and Krebs cycle intensities were also simulated only in highly simplified form. The phenomena of proton leak and of the Each Step Activation were integrated into the model. The model implements Each Step Activation intensity A_{OX} assuming a saturating-type A_{OX}-A_{UT} dependence:

$$A_{OX} = 1+A_{OX_{Max}}\left(\frac{A_{UT} - 1}{(A_{UT} - 1) + K_{A_{UT}}}\right)$$

($A_{OX_{Max}}$=5, $K_{A_{UT}}$=5), as it was shown to more accurately describe volunary muscle performance (Korzeniewski, 2018). Furthermore, the activities of lactate dehydrogenase, creatine kinase, and adenylate kinase were also acknowledged together with the pools of the corresponding metabolites. For simplicity and to make possible simulations of the stationary states of metabolite concentrations, the phenomenon of the slow-component increase in ATP consumption, as well as the activities of AMP deaminase and complex II, were excluded from this version of the model. Accommodation of metabolite fluxes to the state of exercise (increased ATP consumption) takes time (Korzeniewski, 2015; Korzeniewski, 2018); therefore, data on metabolite concentration are collected from time points after steady state is achieved. In this study, conservative time delay of around 24 min after the start of exercise was adapted, as the preliminary simulations showed that at this point for various simulations the steady state is achieved. The model applied in this research comes from the 'cortically stimulated skeletal muscle' version of the model used by Korzeniewski (Korzeniewski, 2018).

The mathematical model was implemented in the form of the Fortran (Fortran 77) program shared by Prof. Korzeniewski. To simulate changes in metabolite concentrations, the GEAR Method subroutine was used as the algorithm for differential equation solving (based on Gear 1971). By applying the Gear method, the problems posed by the stiffness of the simulated system were avoided, and higher accuracy and precision were obtained due to the autoregulation of the time step of simulation (usually between 10^{-4} and 10^{-3} min).

Intermediate states for the activity of ETC complexes I and III, ATP synthase, phosphate carrier, and creatine kinase are modeled only in simplified form with the use of thermodynamic span parameters. For them, kinetic description could be simplified as they work close to thermodynamic equilibrium (Korzeniewski, 2017; Rohwer & Hofmeyr, 2010), in case of the rest of modeled enzymes which work far from equilibrium, the forward reaction rates are thousand to millions of times faster than backward rates, so the model also simplifies description to the forward reactions (Korzeniewski, 2017) (for exact equations and rate constants values see Appendix at https://ojs.ptbioch.edu.pl/index.php/abp/). In this work, stationary states of metabolite concentrations were analyzed that formed after more than 15 min of accommodation of metabolite fluxes to the new increased level of ATP usage (state of exercise), so the effects of model simplifications (with regard to intermediate stages of enzyme activity) on such concentration values should be marginal. Further information about the model and limits of its application can be found in the Appendix at https://ojs.ptbioch.edu.pl/index.php/abp/ and in the cited literature (Korzeniewski, 2011; Korzeniewski, 2017; Korzeniewski, 2018; Korzeniewski & Rossiter, 2015; Korzeniewski & Zoladz, 2015).

Through modifications of the model parameters (enzymatic/transporter activity constants), the states of various mitochondrial dysfunctions were mimicked and the flux of metabolites in skeletal muscle was simulated. To model mitochondrial dysfunctions of various degrees of severity, the simulations cover an array of states of decreasing (from 100% to 10%, with 10% interval) activities of mitochondrial ETC complexes (CI, CIII, CIV), ATP synthase (SN), phosphate transporter (PI), and of the ATP/ADP exchanger (EX). States of decreased activity were achieved through the multiplication of the corresponding enzymatic/transporter activity rate constant(s) (k_{CI}, k_{C3}, k_{C4}, k_{SN}, k_{EX}, k_{PI}; see Appendix at https://ojs.ptbioch.edu.pl/index.php/abp/) by the target percent value. As this model mimics an *average* from the system of proteins in the muscle, the effect of decrease of given protein activity rate constant may have (at least) a trifold interpretation: 1) Corresponding gene mutations lead to the perturbation of protein(s) structure and concomitantly of its enzymatic/transporter activity by a given percentage number; 2) Given percent of corresponding protein(s) is inactive (e.g. damaged by oxygen species); 3). Certain process (i.e. defects of mitochondrial protein synthesis and complex assembling mechanisms) leads to the decreased quantity of functional protein(s) particles in the cell (or adequate compartment). The decrease in the number of mitochondria in the cell also falls in the third scenario. Obviously, another possibility is the combination of all three phenomena, which results in a given average decrease in the rate of transformation or translocation of metabolites.

The oxygen consumption rate ($\dot{V}O_2$), pH and the changes of concentrations of ATP, ADP, phosphate (Pi), and phosphocreatine (PCr) concentrations were monitored in their stationary states for various muscle workloads at the time point of where metabolite fluxes were accommodated to the state of the given workload. The workloads were simulated and measured as the magnitudes of ATP consumption at rest (A_{UT}) spanning from 10 to 100 with an interval of 10. Additional simulations were conducted for the state of rest (A_{UT}=1). Applying Python (Python 2.7, with the Matplotlib module), the data obtained from the simulations of all (>800) combinations of dysfunction variants, degree of severity, and workload intensity were explored, sorted, and expressed in the form of series of workload-dependence or activity-decrease-dependence plots.

A series of additional simulations allowed to estimate such threshold levels of OXPHOS impairment for given workloads (in the range of A_{UT} between 10 and 100), which generate critical levels of accumulation of Pi or H^+ (that is: [Pi] = 25 mM and pH = 6.6). Further simulations with modified concentrations of magnesium ions (up to ±15%) enabled the evaluation of the potential additional role of this factor in the aforementioned variants of mitochondrial dysfunctions.

RESULTS

The comparisons in Fig. 1A–B illustrate the workload-activity impairment thresholds of the models of impairment of complexes I, III and IV, ATP synthase, ATP/ADP exchanger and the phosphate carrier. Additionally, the curve for the impairment of all those elements is shown together with the curve for the analogous model, where only the activity of EX is fully preserved. Each point on the curve represents the workload threshold value for a given degree of OXPHOS impairment. The range of applied workloads (A_{UT} from 10 to 100) forms a representative palette of various situations in everyday life. Higher intensities do occur, however, mostly in the time of the highest intensity athletic performance and

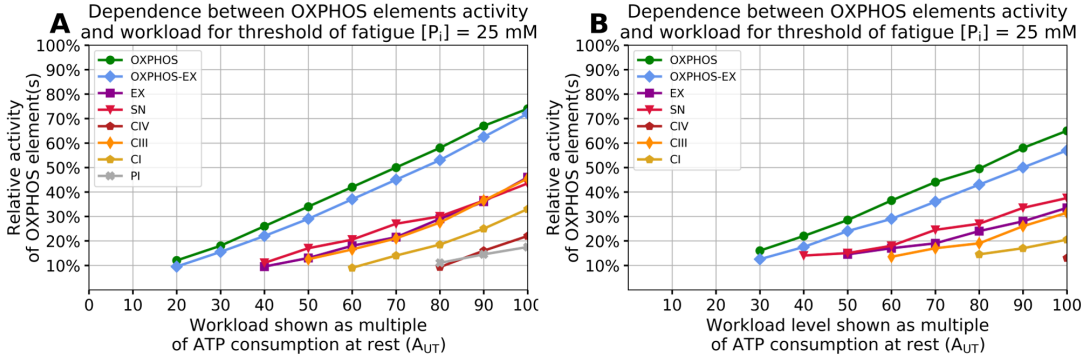

Figure 1. Dependency between workload and degree of remaining activity of OXPHOS elements for threshold of fatigue in form of: (**A**) 25 mM cytoplasmic phosphate concentration, or (**B**) cytosol acidification to pH of 6.6. A_{UT} – multiple of ATP usage at rest OXPHOS – model for proportional impairments of whole OXPHOS system, OXPHOS-EX – simulation for impairment of every component of OXPHOS except for ATP/ADP exchanger, SN – ATP synthase, PI – phosphate transporter, CI-IV – complexes of electron transport chain. There are no pH = 6.6 thresholds workload-activity values for PI in the range of simulated conditions.

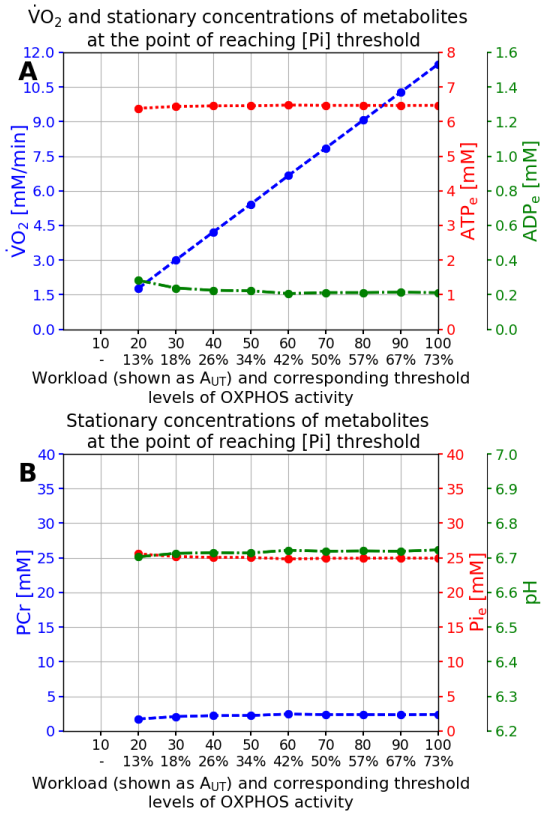

Figure 2. Concentrations values of metabolites at the point of reaching threshold phosphate concentration for the model of entire OXPHOS dysfunctions (for the points shown in Fig. 1A).
Values for threshold pairs of workload (shown as A_{UT}) and level of OXPHOS activity (shown as rounded percentage of basal value) A – $\dot{V}O_2$ and stationary ATP and ADP concentrations, B – pH and concentrations of phosphate and phosphocreatine. A_{UT} – multiple of ATP usage at rest, – $\dot{V}O_2$ oxygen consumption rate, PCr – phosphocreatine, Pi_e – cytosolic phosphate concentration.

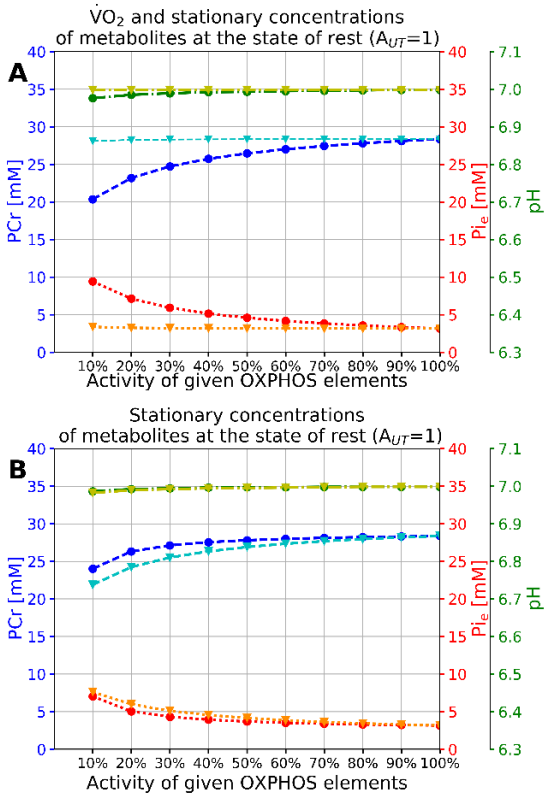

Figure 3. Simulations of muscle in the state of rest (A_{UT} = 1) for various degrees of impairment of the entire OXPHOS (dots, red, blue dark green) or Complex III (triangles, orange cyan, light green).
Oxygen consumption rate and stationary concentrations of metabolites in models of increasing activities of OXPHOS. **Abbreviations**: A_{UT} – multiple of ATP usage at rest, $\dot{V}O_2$ – oxygen consumption rate, PCr – phosphocreatine, Pi_e – cytosolic phosphate concentration.

probably only for timespans of seconds (Korzeniewski, 2019). For comparison, the workload at the levels of $A_{UT} \cong 35$ corresponds to moderate intensity exercise, above the level of 50 A_{UT}, it corresponds to the exercise of heavy or severe intensity (e.g. at 80 A_{UT}) (Korzeniewski, 2018; Korzeniewski, 2019). Additional simulations for the workload of even higher intensity for the whole OXPHOS dysfunction model result in critical impairment values rising roughly linearly. In time of exercise for intact basal (100%) OXPHOS activities, the 25 mM phosphate thresholds are acquired for workloads slightly above 127 A_{UT} (not shown). It should be noted that, at the point of the phosphate threshold at the level of basal OXPHOS activities, the curves of all the dysfunction models cross with each other. This is an obvious observation as there must exist some common starting point for all these curves, in which all OXPHOS are intact. For workloads greater than A_{UT} = 100 the threshold activity values for the curves for single-disfunction models increase exponentially (roughly) to reach that 'starting point' of ~127 A_{UT} (not shown). In example, for the PI dysfunctions the activity threshold rises sharply reaching 50% at 120 A_{UT} workload and leaps by remaining 50% in the span of the further 7 A_{UT} units of additional workload. All of these workloads above 100 A_{UT} are theoretically achievable. However, in a practical sense it is possible only in the time of extreme intensity athletic performance, probably mostly for well-trained (or talented) professionals (Korzeniewski, 2019).

As shown in Fig. 1A, the highest threshold values (the earliest to cross) exist in the model of whole OXPHOS impairment, next is the entire OXPHOS impairment model with the exception for fully efficient EX. The impairments of EX, SN, and CIII give threshold curves similar to each other. Lower threshold values were observed for CI followed by CIV. The phosphate carrier (PI) impairment model even for the highest threshold workloads gives the lowest impairment values. In that case, fatigue thresholds are reached only for the most severe cases of activity impairment and for the most severe workloads.

In the case of an increase in acidity to pH 6.6 (Fig. 1B) serving as a threshold, the order of severity of impairments for each OXPHOS element is identical to that for phosphate, but threshold values are reached for more severe workloads and activity impairments than in the case of thresholds for phosphate concentrations. The next figure (Fig. 2) illustrates the stationary concentrations of metabolites at each of the phosphate threshold reaching points in Fig. 1A. It should be noted that the concentrations of each metabolite are roughly equal between various threshold points. Of particular importance is the pH, which seems to be between values of 6.75 and 6.70 for all models with OXPHOS intensity levels above 20%. For levels of OXPHOS intensity less than 60%, the pH appears to decrease slightly with increasing level of OXPHOS impairment, crossing the pH level of 6.7 for impairment below ~20% of the basal OXPHOS intensity.

The only parameter that differs greatly for all these points is the oxygen consumption rate, which exhibits a linear dependence on the OXPHOS efficiency.

Comparison of the impact of various types of OXPHOS impairments on the stationary concentrations of metabolites in the state of rest ($\mathcal{A}_{UT} = 1$) depicted in Fig. 3 shows that mitochondrial dysfunctions are also capable of increasing the basal concentrations of phosphate in the state of rest. The increase in [P_i] is the most pronounced in the case of dysfunctions that affect the entire OXPHOS (enzymatic/transporter activities of all elements equally affected) (Fig. 3A red). The decrease in the activities of the ATP/ADP exchanger (Fig. 3B orange) and (to a lesser extent) of ATP synthase (Fig. 3A orange) results in similar perturbations. An important observation is that changes for the OXPHOS-EX model of the entire OXPHOS impairment but with the exception for the fully functional EX (Fig. 3A, orange) increase the basal levels of phosphate *less* than in the case of the model of the sole impairment of EX (Fig 3B, orange *vs.* red) with all the other elements fully active. In the case of other single-protein-disruption models (not shown), the increase in stationary concentrations was minuscule. Among the concentrations of other metabolites, there is little to no change except for phosphocreatine, the concentration of which (stationary levels) decreases in a synchronized manner with accumulations of phosphate in response to increasing OXPHOS impairment. In the most severe cases of OXPHOS impairment, there is also a visible marginal decrease in pH (Fig. 3A dark green).

The changes in stationary metabolite concentrations with the level of impairment of a given OXPHOS element are similar between various single protein disruption (or deficiency) models. The most complicated are changes in stationary ADP concentrations in the cases of higher workloads (Fig. 4C, 5B, 5C). In the stages/cases of higher OXPHOS impairment, the ADP levels start to increase sharply with the deterioration of the efficiency. Then there exists the stage of impairment that produces the peak of the stationary [ADP] for the given work intensity. After that point, the stationary ADP concentrations decrease with further deterioration of the OXPHOS intensity but at a slower rate. This effect is more visible for higher workloads and in models of complete OXPHOS impairment in which the ADP peaks for higher OXPHOS activities (Fig. 4C).

Changes in the rate of oxygen consumption and concentrations of ATP and ADP are the most pronounced for impairments affecting the intensity of the entire OXPHOS intensity (Fig. 4A, B, C blue, red, dark green). Next are the effects of SN dysfunctions (Fig. 5A, B, C, blue, red, dark green), followed by those for EX (Fig. 5A, B, C, cyan, orange, light green) which are slightly higher than those for CIII (Fig. 4A, B, C, cyan, orange, light green). The effects increase with increasing workload (A, B, C). Parallel results occur for the pH and concentrations of phosphate and phosphocreatine (A', B', C'). The effects of impaired CI and CIV are less severe, and for the PI visible changes occur only at the time of the most severe workloads (Not shown). In the model in which the efficiencies of all OXPHOS elements except EX are interrupted, the changes of the stationary concentrations and of the oxygen consumption rate are moderately lowered compared to the entire OXPHOS impairment model (Fig. 6A).

The course of the ATP dependence on OXPHOS efficiency is sigmoidal, and at a certain point, the stationary ATP concentration starts to decrease greatly with the further decrease of the OXPHOS element(s) activity (Fig. 4C, Fig. 5C). For the most severe impairments and the highest workloads, the decrease in stationary ATP concentrations reaches such low levels that it may interfere even with the constitutive functioning of myocytes. A similar, partially sigmoidal dependence could be observed, in the cases of a higher workload or levels of OXPHOS impairments, also for pH and stationary phosphate concentrations (Fig. 4B', 4C', 5C'). However, for lower workloads or levels of OXPHOS impairment, that sigmoidal dependence is

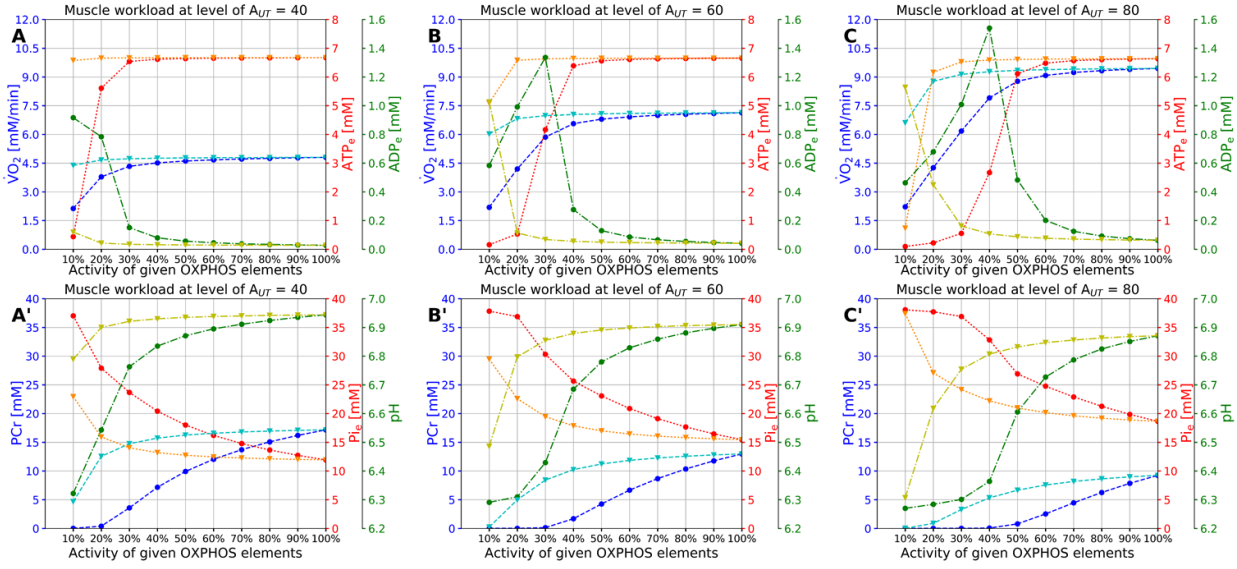

Figure 4. Simulations of working muscle in given workload conditions (A 40 A_{UT}, B 60 A_{UT}, C 80 A_{UT}) for various degrees of impairment of the entire OXPHOS (dots, red, blue dark green) or Complex III (triangles, orange cyan, light green)
A, B, C – $\dot{V}O_2$ and stationary ATP and ADP concentrations, A', B', C' – pH and concentrations of phosphate and phosphocreatine. Stationary concentrations of metabolites in models of increasing activities of OXPHOS. **Abbreviations**: A_{UT} – multiple of ATP usage at rest, $\dot{V}O_2$ – oxygen consumption rate, PCr – phosphocreatine, Pi_e – cytosolic phosphate concentration.

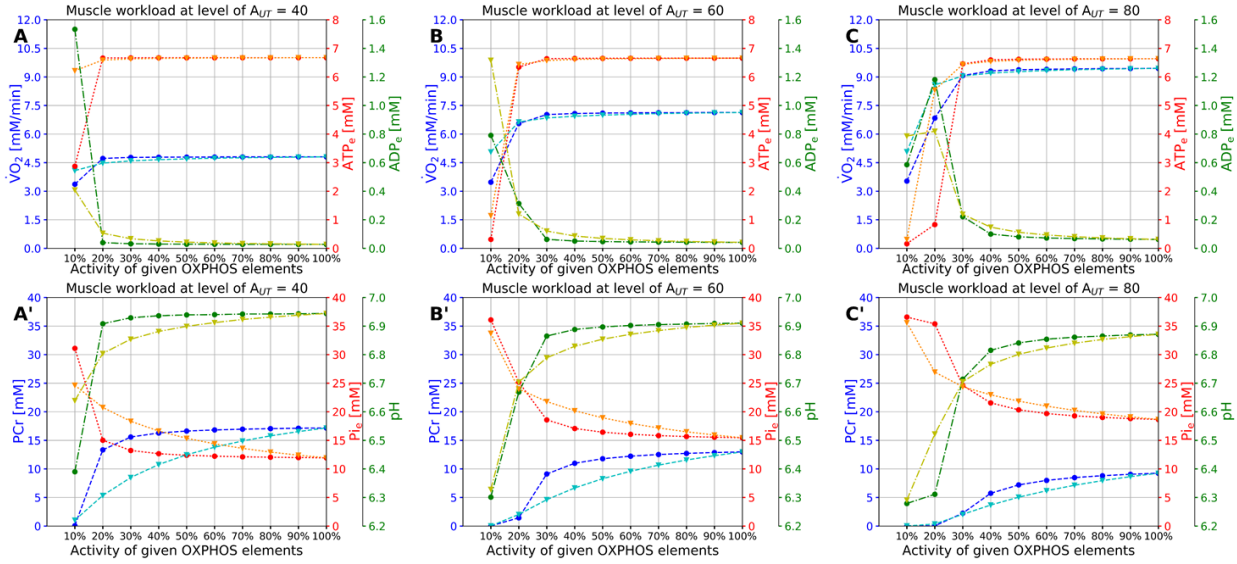

Figure 5. Simulations of working muscle in given workload (A 40 A_{UT}, B 60A_{UT}, C 80 A_{UT}) conditions for various degrees of impairment of ATP synthase (SN) (dots, red, blue dark green) or ATP/ADP exchanger (EX) (triangles, orange cyan, light green)
A, B, C – $\dot{V}O_2$ and stationary ATP and ADP concentrations, A', B', C' – pH and concentrations of phosphate and phosphocreatine. Oxygen consumption rate and stationary concentrations of metabolites in models of increasing activities of OXPHS elements. **Abbreviations**: A_{UT} – multiple of ATP usage at rest, $\dot{V}O_2$ – oxygen consumption rate, PCr – phosphocreatine, Pi_e – cytosolic phosphate concentration.

not visible due to its shift to lower levels of OXPHOS activities (Fig. 4A). The collapse of pH and stationary concentrations of phosphate and ATP appears to be correlated with the peaks of ADP concentrations (Fig. 4A', 5A', B'). Comparison between the entire OXPHOS impairment model and its equivalent with fully active EX shows that the sole unimpeded functioning of EX changes the point of collapse of ATP by approximately 10 A_{UT} units (Fig. 6A) or by an additional ~10% of the basal activity (not shown). A similar effect is observed for the accumulation of phosphate, the decrease in pH, and the peak of

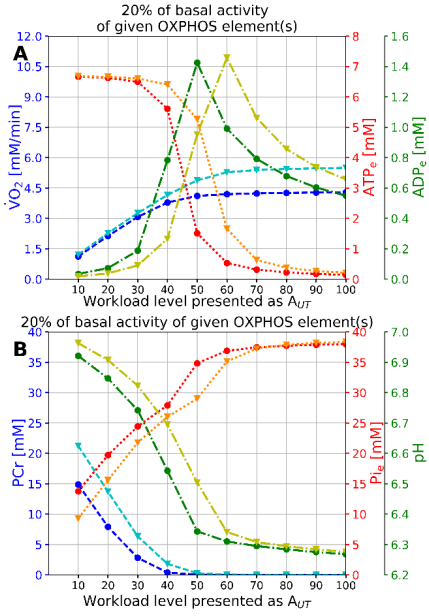

Figure 6. Simulations of muscles working at various workloads at a given level of impairment of the entire OXPHOS (dots, red, blue dark green) or entire OXPHOS except for fully functional ATP/ADP exchanger (OXPHOS-EX model) (triangles, orange cyan, light green).
A – $\dot{V}O_2$ and stationary ATP and ADP concentrations, B – pH and concentrations of phosphate and phosphocreatine. Oxygen consumption rate and stationary concentrations of metabolites in models of increasing workload. **Abbreviations**: A_{UT} – multiple of ATP usage at rest, $\dot{V}O_2$ – oxygen consumption rate, PCr – phosphocreatine, Pi_e – cytosolic phosphate concentration.

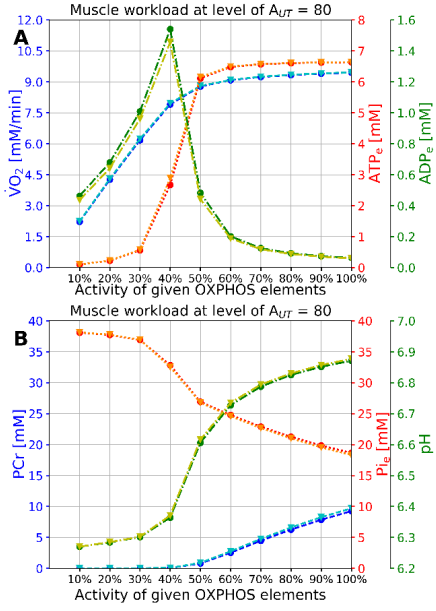

Figure 7. Impact of magnesium ions on stationary concentrations of metabolites in the models of impairment of entire OXPHOS without (dots, red, blue dark green) and with decreased (–15%) concentration of magnesium (triangles, orange, cyan, light green)
A – $\dot{V}O_2$ and stationary ATP and ADP concentrations, B – pH and concentrations of phosphate and phosphocreatine. **Abbreviations**: A_{UT} – multiple of ATP usage at rest, $\dot{V}O_2$ – oxygen consumption rate, PCr – phosphocreatine, Pi_e – cytosolic phosphate concentration.

stationary concentrations of ADP. For higher activities of the OXPHOS elements, before the collapse of ATP levels, the increase in phosphate levels appears to be correlated with a gradual decrease in phosphocreatine concentrations.

Additional simulations with Mg^{2+} concentrations decreasing (Fig. 7) or increasing (not shown) by up to ±15% indicate that changes in the availability of this ion have a minor effect on the concentration of other metabolites. Changes in pH and $[P_i]$ are negligible; the only potentially significant effect is a slight change in [ADP] (Fig. 7A dark green *vs.* light green). The accumulation of Mg^{2+} and ADP exhibits the inverse correlation: increasing cellular Mg decreases slightly the concentration of ADP. Comparing the impact in various dysfunction models, this effect is the most visible in the case of impairments of the whole OXPHOS. However, apart from the scale of effects, there are no other differences between normal and low magnesium variants for any of the impairments of OXPHOS elements.

DISCUSSION

Among mitochondrial dysfunctions, exercise intolerance is a widely coexisting symptom. It occurs both in the entire OXPHOS dysfunctions and in the dysfunctions that impair only one element of the OXPHOS. The former group encompasses dysfunctions such as MELAS or MERRF that stem from mutations in mitochondrial tRNA coding genes. Such mutations simultaneously impair the production of various OXPHOS proteins and in some cases they are related to vulnerability to fatigue (Mancuso *et al.,* 2012). Among the dysfunctions that selectively alter one element of OXPHOS as a curios example stand the effects of G14846A mutations of the *Cytb* gene, which impair the functioning of Complex III of ETC (Andreu *et al.,* 1999). Such mutations result in the so-called 'Pure Exercise Intolerance', in which vulnerability to fatigue is the only symptom. For obvious reasons, such dysfunctions may be hard to diagnose, and their true prevalence in the population could be underestimated. As another example, it may serve to define the disfunctions connected with impairment of mitochondrial transporters. For dysfunctions of EX, also known as the adenine nucleotide transporter – ANT, few types of related diseases such as some variants of CPEO (Chronic progressive external ophthalmoplegia) were reported (Bakker *et al.,* 1993; Palmieri *et al.,* 2005; Strauss *et al.,* 2013), vulnerability to fatigue was listed as one of the symptoms of such diseases. The extreme example of single OXPHOS element impairments is the c.158-9A>G mutation of the mitochondrial phosphate transporter (PI) gene. As this mutation affects only the muscle-specific isoform, symptoms of this disease are limited to skeletal and heart muscles, including exercise intolerance and hypertrophic cardiomyopathy, other mutations in the same gene result in death within the first years of life (Bhoj *et al.,* 2014). The progression of symptoms (including exercise intolerance) is a common aspect that occurs in some cases of mentioned mitochondrial dysfunctions of both types (entire-OXPHOS impairments and single OXPHOS element dysfunctions). This was one of the reasons why simulations were conducted for a whole spectrum of percentage activity impairments. As explained (see Introduction), this spectrum of activities could also describe situations of increasing mutation load (unfunctional mitochondria load) of cells.

To confront simulations with empirical data, corresponding empirical results from the literature were analyzed. In the work: "The spectrum of exercise tolerance in mitochondrial myopathies: a study of 40 patients" Taivassalo and others (Taivassalo *et al.*,, 2003) investigated the power output of patients with myopathies, most of the cases pertained to the category of entire OXPHOS mutations such as Kearns–Sayre syndrome or mitochondrial encephalomyopathy (tRNAleu 3243 mutation). Taivassalo also obtained data on the percentage of mutation load in these patients. According to one of the given interpretations (see Introduction), in the case of entire OXPHOS mutations, this percentage of mutation load could be roughly equivalent to the degree of *loss of* OXPHOS activity. For almost all patients, the mutation load values were between roughly 35% and 100%. The maximum $\dot{V}O_2$ was equal to about 25–27.5 ml/min per kilogram of body mass (Taivassalo *et al.,* 2003). The average weight of the patients was 65 kg, which means that the maximum oxygen consumption rate was approximately between 7.25 and 8 mmol/min. According to Fig. 2, where $\dot{V}O_2$ at the level of reaching the phosphate threshold, such values are achieved for the level of impairment equal to approximately 47–52% of the basal OXPHOS activity. This is somewhat lower than the values stated in the work of Taivassalo and others (Taivassalo *et al.,* 2003) where, according to the approximation mentioned above, myopathic patients with *up to* 65% of normal OXPHOS activity were tested. Considering the variety of the mitochondrial heteroplasmic dysfunctions group, mutation load-activity approximation, and the fact that in these simulations $\dot{V}O_2$ (and thus also the levels of corresponding threshold of OXPHOS activity) are slightly underestimated, because of the omission of the slow component (see Methods), it could be seen that the model gives performance barriers posed by fatigue rather similar to the empirical results, at least in the case of their entire-OXPHOS variants such as CPEO, MELAS and other, especially mitochondrial tRNA related, dysfunctions.

The results of the simulations show that for models of entire OXPHOS dysfunctions, the correlation between workload and threshold OXPHOS impairment is nearly linear (Fig. 1A). This linearity may be interpreted as an illustration of evolutionary fine-tuning of the activities of every OXPHOS element. When all rates change proportionally, there is no additional (i.e., extra proportional) accumulation of metabolites. This model of entire-OXPHOS impairment could also be seen as equivalent to the situation of a depleted number of mitochondria in the cell. For models of single protein dysfunctions, the impaired flux of electron carriers and metabolites leads to additional disturbances for the system, thus its 'output' becomes non-linear, hence, for some workloads, stationary concentrations change faster in response to impairments of single OXPHOS elements. However, in the investigated range of workloads, these changes are not as pronounced as in the case of the entire-OXPHOS-wide impairments. The models ordered according to the severity of the effects of impairment on phosphate-induced fatigue are as follows: SN>EX≥CIII>CI>CIV>PI. A stationary Pi concentration of 25 mM was assumed as the critical concentration, as other modeling works have shown that this concentration is sufficient to give fatigue simulation results consistent with empirical critical power measures (Korzeniewski, 2019). However, comparison of stationary metabolite concentrations at the point of crossing the phosphate concentration threshold for various combinations of workload and degree of OXPHOS

impairment (Fig. 2) suggests that acidity thresholds seem to always be reached slightly later than those of phosphate. As Fig. 2B shows, the crossing of the phosphate threshold always occurs at pH values of approximately 6.7–6.75, while minimal acidity thresholds related to fatigue are below the pH of 6.7 (Fitts, 2008). According to the simulations, to reach a pH equal to 6.6, which should result in bold fatigue-leading effects of acidity, the activity rates of the OXPHOS elements must be further reduced by approximately 7–10% relative to the phosphate thresholds. Alternatively, the ATP consumption rate would need to be increased by a similar A_{UT} value. Taking into account the 'vicious cycle' effect of the slow component present in the real working muscle (Korzeniewski, 2019), this means that the effects of reaching both thresholds should dynamically blur one into another. Therefore, in real working muscle, in most cases, there is probably little to no visible biphasic effect of phosphate and acidity on fatigue. However, this model simulates 'averaged' skeletal muscle, while there exist differences between various types of muscle fibers. This could explain why in some experiments, at the time of fatigue, pH levels of muscle fiber were reported to be as low as 6.2 (Sundberg *et al.,* 2019).

Another factor that influences fatigue, which has its own and distinct mechanisms of action, is magnesium. However, the results of the simulations rule out any significant additional cross-interactions that impact acidity build-up or phosphate accumulation (Fig. 7B). Even bold disturbances (±15%) of total magnesium concentrations cannot increase the build-up of these metabolites. Slight changes in the levels of cytoplasmic [ADP] are the only visible effects of these disturbances. Changes in total intercellular magnesium concentrations of up to 15% were reported; however, in normal conditions free magnesium pools constitute only a minor fraction of total magnesium in the cell (Murphy, 2000). On the other hand, in the model applied here, the significant part of those elevated magnesium ion concentrations is also rapidly utilized by the formation of complexes with ATP or ADP. Although the effects of these interactions are visible, their minuscule scale appears to rule out any significant impact of magnesium accumulation on the accumulation of fatigue-leading metabolites through any of the pathways acknowledged in this model. However, magnesium could also affect the process of fatigue through other indirect mechanisms (listed in the Introduction). Furthermore, magnesium ions may possibly influence the fatigue process at the level of interactions with the effects of Pi or H^+ accumulation on the energetic efficiency of muscle contractions. However, this process is not directly included in this model (these effects might only be indirectly acknowledged as part of the resultant slow component if that element is present in the model).

Concentrations of phosphate and acidity are the main topic of this research. However, ADP peaks raise the question of the eventual role of this metabolite in the fatigue process. In fact, some works propose ADP as yet another fatigue-leading agent. Experimental research shows that there is a detrimental effect of higher ADP concentrations on the speed of single myosin protein movement along the actin filament (Allen *et al.,* 2008), but this was shown not to result in impaired macroscopic muscle contractions or decreased ability to generate force in that process (Greenberg *et al.,* 2010; Debold 2012).

Among the OXPHOS elements investigated, the ATP/ADP exchanger was surprisingly identified as one of the crucial elements to stabilize phosphate concentrations, both in the state of rest and during exercise. In times of increased workload, impairment of EX demonstrated effects greater than those of some of the ETC complexes and comparable with those of such crucial OXPHOS enzymes as the ATP synthase and Complex III. In fact, empirical results exist that agree with this predicted major role of the ATP/ADP exchanger for oxidative phosphorylation; (Willis *et al.,* 2018), however, those experiments were conducted on mitochondria isolated from muscles and not in living, working muscle, while experiments on isolated mitochondria were shown to not accurately reflex the metabolite fluxes of the working muscle (Korzeniewski, 2015; Korzeniewski, 2016). In contrast to EX, the role of PI, the phosphate (and H^+) carrier, turned out to be nearly negligible. This is a rather unintuitive finding, as this protein is involved in the direct transport, between the cytoplasm and mitochondria, of crucial metabolites in the fatigue process. In fact, as the simulations suggest, its activity appears to be fully sufficient against fatigue, whereas the bottleneck of the phosphate utilization pathways appears to lie in the production of ATP from ADP and phosphate by ATP synthase and in the effective exchange of both nucleotides between the mitochondria and the cytosol by EX.

Of great importance could be the further results for the model of impairment of the whole OXPHOS with the exception of a fully functional EX. This protein is much smaller and consists of only one type of unit in opposition to the other OXPHOS complexes. With all of the above considered, this may suggest that among future gene therapy approaches against mitochondrial dysfunctions, the ATP/ADP exchanger may be one of the first targets of choice. In fact, such interventions had already been shown to be possible in the mouse model (Flierl *et al.,* 2005). Furthermore, the literature suggests a great role for the EX in the process of ageing, especially for age-related weakening of the muscles (Yan & Sohal, 1998; Gouspillou *et al.,* 2010; Diolez *et al.,* 2015). This is also related to the reported vulnerability of this protein to oxidative damage (Yan & Sohal, 1998). Such an OXPHOS disruption process through oxidative impairment of EX in the time of higher workloads may also serve as a partial explanation for the various works suggesting the beneficial effect of antioxidants on athletic performance (Reid, 2016; Thirupathi & Pinho, 2018). Indeed, various empirical works support the non-negligible role of EX for the ability to maintain muscle work. For example, there are known mitochondrial diseases that are caused by mutations in the genes that encode the EX protein. Among their symptoms, vulnerability to fatigue and myopathies was reported (Bakker *et al.,* 1993; Palmieri *et al.,* 2005; Strauss *et al.,* 2013). There also exist toxins dangerous to humans that target the ATP/ADP exchanger, such as bongkrekic acid (Anwar *et al.,* 2017). Finally, existing reports suggest the crucial role of the diversity of muscle-type-specific prevalence of EX isoforms. This phenomenon may be partially related to the unique properties of extraocular muscles extremally resistant to fatigue of the eyeball that, unlike other skeletal muscles, also express the ANT2 isoform of EX (Fuchs & Binder, 1983; Yin *et al.,* 2005; Liu & Chen, 2013). In the model applied in this research, only one form of the EX is acknowledged. Its activity is the statistical average of the effects of various proportions of isoforms in the same way that the whole model was gradually constructed to recreate the performance of the entire muscle, not the specific types of its fibers. This also suggests possible ways for the model to be further developed. that

would enable the simulation of those specific types of muscle fibers.

In summary, the present study shows possible effects of mitochondrial dysfunctions that can lead to accumulation of fatigue-leading metabolites: phosphate and H^+ ions. From the perspective of vulnerability to fatigue, it also tries to describe differences in the spectra of severity and in possible progression trajectories in both types of such diseases: those affecting one OXPHOS elements, e. g. pure exercise intolerance syndrome in case of *cyth* mutations and those affecting the entirety of OXPHOS like in the case of large mtDNA deletions leading to CPEO or in MELAS cases related to mutations in mitochondrial tRNA encoding genes. In entire OXPHOS disfunction models, the dependence between workload and level of OXPHOS activity leading to phosphate threshold is linear, and in case of single-OXPHOS-element models it is exponential with threshold workload/activity levels lower than in the case of dysfunctions impacting entire OXPHOS. Simulation results also suggest that the crossing of phosphate accumulation thresholds always precedes the reaching of those for acidity, but also that time separation between these two processes is probably minimal. The results of additional simulations show that eventual perturbations of concentrations of another factor related to fatigue – magnesium ions – are unable to change the course of cytosolic phosphate and H^+ accumulation in any of the investigated models of OXPHOS interruption. A comparison of various models of OXPHOS deficiency rules out any possible leading role of the phosphate carrier in the fatigue process in the scope of the presented workloads. However, in this investigation, the ATP/ADP exchanger has been shown (Fig. 3B, 4A'4B'C') to be a crucial factor in preventing the accumulation of phosphate and [H^+] with the effects of its disruption on a par with the effects of ATP synthase or complex III impairments. The model shows that EX activity is also the main factor that regulates cytosolic concentrations of phosphate at rest (Fig. 3B) with the effect of disruption greater than the equivalent effects of simultaneous decrease of all other OXPHOS elements activity by the same percent value.

Acknowledgements

The mathematical and computer models of the bioenergetic pathways of skeletal muscle were kindly shared by Prof. Bernard Korzeniewski, who was also the supervisor of the author's master thesis: *"Theoretical studies on the influence of oxidative phosphorylation deficiencies and exercise intensity in skeletal muscle on the respiration rate, and metabolite concentrations in the context of muscle work termination because of fatigue"*, on which the main part of this article is based. The mathematical model shared by Prof. Bernard Korzeniewski is freely available on the website: http://awe.mol.uj.edu.pl/~benio/models.html [accessed 9 July 2022].

Declatarions

Conflict of interest statement. Author declares that he has no competing interests.

REFERENCES

Allen DG, Lamb GD, Westerblad H (2008) Skeletal muscle fatigue: cellular mechanisms. *Physiol Rev* **88**: 287–332. https://doi.org/10.1152/physrev.00015.2007

Andreu AL, Hanna MG, Reichmann H, Bruno C, Penn AS, Tanji K, Pallotti F, Iwata S, Bonilla E, Lach B, Morgan-Hughes J, DiMauro S (1999) Exercise intolerance due to mutations in the cytochrome b gene of mitochondrial DNA. *N Engl J Med* **341**: 1037–1044. https://doi.org/10.1056/NEJM199909303411404

Anwar M, Kasper A, Steck AR, Schier JG (2017) Bongkrekic acid —a review of a lesser-known mitochondrial toxin. *J Med Toxicol* **13**: 173–179. https://doi.org/10.1007/s131810160577

Bakker HD, Scholte HR, Van Den Bogert C, Ruitenbeek W, Jeneson JAL, Wanders RJA, Abeling NGGM, Dorland B, Sengers RCA, Van Gennip AH (1993) Deficiency of the adenine nucleotide translocator in muscle of a patient with myopathy and lactic acidosis: a new mitochondrial defect. *Pediatr Res* **33**: 412–417. https://doi.org/10.1203/00006450-199304000-00019

Bhoj, EJ, Li, MC, Ahrens-Nicklas, RC, Pyle LC, Wang, J, Zhang, VW, Clarke CF, Wong LC, Sondheimer N, Ficicioglu, C, and Yudkoff, M (2015) Pathologic variants of the mitochondrial phosphate carrier SLC25A3: two new patients and expansion of the cardiomyopathy/skeletal myopathy phenotype with and without lactic acidosis. *JIMD Rep* **19**: 59–66. https://doi.org/10.1016%2Fj.bbrc.2015.06.031

Cheng AJ, Place N, Westerblad H (2018) Molecular basis for exercise-induced fatigue: the importance of strictly controlled cellular Ca^{2+} handling. *Cold Spring Harb Perspect Med.* **8**: a029710. https://doi.org/10.1101/cshperspect.a029710

Debold EP (2012) Recent insights into the molecular basis of muscular fatigue. *Med Sci Sports Exerc* **44**: 1440–1452. https://doi.org/10.1249/MSS.0b013e31824cfd26

Debold EP, Longyear TJ, Turner MA (2012) The effects of phosphate and acidosis on regulated thin-filament velocity in an in vitro motility assay. *J Appl Physiol* **113**: 1413–1422. https://doi.org/10.1152/japplphysiol.00775.2012

Debold EP, Fitts RH, Sundberg CW, Nosek TM (2016) Muscle fatigue from the perspective of a single crossbridge. *Med Sci Sports Exerc* **48**: 2270–2280. https://doi.org/10.1249/MSS.0000000000001047

Diolez P, Bourdel-Marchasson I, Calmettes G, Pasdois P, Detaille D, Rouland R, Gouspillou G (2015) Hypothesis on skeletal muscle aging: mitochondrial adenine nucleotide translocator decreases reactive oxygen species production while preserving coupling efficiency. *Front Physiol* **6**: 369. https://doi.org/10.3389/fphys.2015.00369

Fitts, RH, (2008) The cross-bridge cycle and skeletal muscle fatigue. *J Appl Physiol* **104**: 551–558. https://doi.org/10.1152/japplphysiol.01200.2007

Flierl A, Chen Y, Coskun PE, Samulski RJ, Wallace DC (2005) Adeno-associated virus-mediated gene transfer of the heart/muscle adenine nucleotide translocator (ANT) in mouse. *Gene Ther* **12**: 570–578. https://doi.org/10.1038/sj.gt.3302443

Fuchs AF, Binder MD (1983) Fatigue resistance of human extraocular muscles. *J Neurophysiol* **49**: 28–34. https://doi.org/10.1152/jn.1983.49.1.28

Gandevia SC (2001) Spinal and supraspinal factors in human muscle fatigue. *Physiol Rev* **81**: 1725–1789. https://doi.org/10.1152/physrev.2001.81.4.1725

Gear CW, (1971) DIFSUB for Solution of ordinary differential equations [D2] (Algorithm 407) *Commun ACM* **14**: 185–190. https://doi.org/10.1145/362566.362573

Gouspillou G, Bourdel-Marchasson I, Rouland R, Calmettes G, Franconi J-M, Deschodt-Arsac V, Diolez P (2010) Alteration of mitochondrial oxidative phosphorylation in aged skeletal muscle involves modification of adenine nucleotide translocator. *Biochim Biophys Acta* **1797**: 143–151. https://doi.org/10.1016/j.bbabio.2009.09.004

Greenberg MJ, Mealy TR, Jones M, Szczesna-Cordary D, Moore JR (2010) The direct molecular effects of fatigue and myosin regulatory light chain phosphorylation on the actomyosin contractile apparatus. *Am J Physiol Regul Integr Comp Physiol* **298**: R989–R996. https://doi.org/10.1152/ajpregu.00566.2009

Hall MM, Rajasekaran S, Thomsen TW, Peterson AR (2016) Lactate: friend or foe. *PM R* **8**: S8–S15. https://doi.org/10.1016/j.pmrj.2015.10.018

Jarvis K, Woodward M, Debold EP, Walcott S (2018) Acidosis affects muscle contraction by slowing the rates myosin attaches to and detaches from actin. *J Muscle Res Cell Motil* **39**: 135–147. https://doi.org/10.1007/s10974-018-9499-7

Kanungo S, Morton J, Neelakantan M, Ching K, Saeedian J, Goldstein A (2018) Mitochondrial disorders. *Ann Transl Med* **6**: 475–475. https://doi.org/10.21037/atm.2018.12.13

Korzeniewski B (2011) Computer-aided studies on the regulation of oxidative phosphorylation during work transitions. *Prog Biophys Mol Biol* **107**: 274–285. https://doi.org/10.1016/j.pbiomolbio.2011.08.003

Korzeniewski B (2015) Effects of OXPHOS complex deficiencies and ESA dysfunction in working intact skeletal muscle: implications for mitochondrial myopathies. *Biochim Biophys Acta* **1847**: 1310–1319. https://doi.org/10.1016/j.bbabio.2015.07.007

Korzeniewski B (2016) Faster and stronger manifestation of mitochondrial diseases in skeletal muscle than in heart related to cytosolic inorganic phosphate (Pi) accumulation. *J Appl Physiol* **121**: 424–437. https://doi.org/10.1152/japplphysiol.00358.2016

Korzeniewski B (2017) Regulation of oxidative phosphorylation through each-step activation (ESA): Evidences from computer

modeling. *Prog Biophys Mol Biol* **125**: 1–23. https://doi.org/10.1016/j.pbiomolbio.2016.12.001

Korzeniewski B (2018) Regulation of oxidative phosphorylation is different in electrically- and cortically-stimulated skeletal muscle. *PLoS One* **13**: e0195620. https://doi.org/10.1371/journal.pone.0195620

Korzeniewski B (2019) Pi-induced muscle fatigue leads to near-hyperbolic power-duration dependence. *Eur J Appl Physiol* **119**: 2201–2213. https://doi.org/10.1007/s00421-019-04204-8

Korzeniewski B, Rossiter HB (2015) Each-step activation of oxidative phosphorylation is necessary to explain muscle metabolic kinetic responses to exercise and recovery in humans. *J Physiol* **593**: 5255–5268. https://doi.org/10.1113/JP271299

Korzeniewski B, Zoladz JA (2015) Possible mechanisms underlying slow component of $\dot{V}O_2$ on-kinetics in skeletal muscle. *J Appl Physiol* **118**: 1240–1249. https://doi.org/10.1152/japplphysiol.00027.2015

Liu Y, Chen XJ (2013) Adenine nucleotide translocase, mitochondrial stress, and degenerative cell death. *Oxid Med Cell Longev* **2013**: 1–10. https://doi.org/10.1155/2013/146860

Mancuso M, Angelini C, Bertini E, Carelli V, Comi GP, Minetti C, Moggio M, Mongini T, Servidei S, Tonin P, Toscano A, Uziel G, Zeviani M, Siciliano G, The Nation-wide Italian Collaborative Network of Mitochondrial Diseases (2012) Fatigue and exercise intolerance in mitochondrial diseases. Literature revision and experience of the Italian Network of mitochondrial diseases *Neuromuscul Disord* **22**: S226–S229. https://doi.org/10.1016/j.nmd.2012.10.012.

Murphy E (2000) Mysteries of magnesium homeostasis. *Circ Res* **86**: 245–248. https://doi.org/10.1161/01.RES.86.3.245

Nelson CR, Debold EP, Fitts RH (2014) Phosphate and acidosis act synergistically to depress peak power in rat muscle fibers. *Am J Physiol Cell Physiol* **307**: C939–C950. https://doi.org/10.1152/ajpcell.00206.2014

Nielsen FH, Lukaski HC (2006) Update on the relationship between magnesium and exercise. *Magnes Res* **19**: 180–189. https://www.jle.com/10.1684/mrh.2006.0060

Palmieri L, Alberio S, Pisano I, Lodi T, Meznaric-Petrusa M, Zidar J, Santoro A, Scarcia P, Fontanesi F, Lamantea E, Ferrero I, Zeviani M (2005) Complete loss-of-function of the heart/muscle-specific adenine nucleotide translocator is associated with mitochondrial myopathy and cardiomyopathy. *Hum Mol Genet* **14**: 3079–3088. https://doi.org/10.1093/hmg/ddi341

Poole DC, Burnley M, Vanhatalo A, Rossiter HB, Jones AM (2016) Critical power: an important fatigue threshold in exercise physiology. *Med Sci Sports Exerc* **48**: 2320–2334. https://doi.org/10.1249/MSS.0000000000000939

Reid MB (2016) Redox interventions and exercise performance. *J Physiol* **594**: 5125–5133. https://doi.org/10.1113/JP270653

Robergs RA, Ghiasvand F, Parker D (2004) Biochemistry of exercise-induced metabolic acidosis. *Am J Physiol Regul Integr Comp Physiol* **287**: R502–R516. https://doi.org/10.1152/ajpregu.00114.2004

Rohwer, JM, Hofmeyr, JH (2010) Kinetic and thermodynamic aspects of enzyme control and regulation. *J Phys Chem B* **114**: 16280–16289. https://doi.org/10.1021/jp108412s

Sharp LJ, Haller RG (2014) Metabolic and mitochondrial myopathies. *Neurol Clin* **32**: 777–799. https://doi.org/10.1016/j.ncl.2014.05.001

Strauss KA, DuBiner L, Simon M, Zaragoza M, Sengupta PP, Li P, Narula N, Dreike S, Platt J, Procaccio V, Ortiz-González XR, Puffenberger EG, Kelley RI, Morton DH, Narula J, Wallace DC (2013) Severity of cardiomyopathy associated with adenine nucleotide translocator-1 deficiency correlates with mtDNA haplogroup. *Proc Natl Acad Sci U S A* **110**: 3453–3458. https://doi.org/10.1073/pnas.1300690110

Sundberg CW, Fitts RH (2019) Bioenergetic basis of skeletal muscle fatigue. *Curr Opin Physiol* **10**: 118–127. https://doi.org/10.1016/j.cophys.2019.05.004

Sundberg CW, Prost RW, Fitts RH, Hunter SK (2019) Bioenergetic basis for the increased fatigability with ageing. *J Physiol* **597**: 4943–4957. https://doi.org/10.1113/JP277803

Taivassalo T, Dysgaard Jensen T, Kennaway N, DiMauro S, Vissing J, Haller RG (20030 The spectrum of exercise tolerance in mitochondrial myopathies: a study of 40 patients *Brain* **126**: 413–423. https://doi.org/10.1093/brain/awg028

Thirupathi A, Pinho RA (2018) Effects of reactive oxygen species and interplay of antioxidants during physical exercise in skeletal muscles. *J Physiol Biochem* **74**: 359–367. https://doi.org/10.1007/s13105-018-0633-1

Willis WT, Miranda-Grandjean D, Hudgens J, Willis EA, Finlayson J, De Filippis EA, Zapata Bustos R, Langlais PR, Mielke C, Mandarino LJ (2018) Dominant and sensitive control of oxidative flux by the ATP-ADP carrier in human skeletal muscle mitochondria: Effect of lysine acetylation. *Arch Biochem Biophys* **647**: 93–103. https://doi.org/10.1016/j.abb.2018.04.006

Woodward M, Debold EP (2018) Acidosis and phosphate directly reduce myosin's force-generating capacity through distinct molecular mechanisms. *Front Physiol* **9**: 862. https://doi.org/10.3389/fphys.2018.00862

Yan L-J, Sohal RS (1998) Mitochondrial adenine nucleotide translocase is modified oxidatively during aging. *Proc Natl Acad Sci U S A* **95**: 12896–12901. https://doi.org/10.1073/pnas.95.22.12896

Yin H, Stahl JS, Andrade FH, McMullen CA, Webb-Wood S, Newman NJ, Biousse V, Wallace DC, Pardue, MT (2005) Eliminating the Ant1 isoform produces a mouse with CPEO pathology but normal ocular motility. *Invest Ophthalmol Vis Sci* **46**: 4555. https://doi.org/10.1167/iovs.05-0695